Table 2.3.4
Details of selected spallation neutron sources

Source	Type	Location	Proton energy	Current	Average power	Target(s)	Repetition rate (Hz)	Moderator(s)
CSNS†	Short pulse	Institute of High Energy Physics, Guangdong, China	1.6 GeV	62.5 μA	100 kW	Tungsten	25	Water, 2 × liquid hydrogen
ESS†	Long pulse	European Spallation Source, Lund, Sweden	2 GeV	2.5 mA	5 MW	Tungsten wheel (helium cooled)	14	2 × Liquid hydrogen (pancake geometry)
ISIS	Short pulse	Rutherford Appleton Laboratory, Oxfordshire, UK	800 MeV	200 μA	160 kW	2 × Tungsten	50	2 × Water, liquid methane, liquid hydrogen
							10	Hydrogen/methane, solid methane at 26 K
JSNS‡	Short pulse	J-Parc Centre, Tokai-mura, Japan	3 GeV	333 μA	1 MW	Liquid mercury	25	Supercritical hydrogen
LANSCE	Long pulse	Los Alamos National Laboratory, Los Alamos, USA	800 MeV	125 μA	100 kW	Tungsten	20	Water, 2 × liquid hydrogen
SINQ	Continuous	Paul Scherrer Institute, Villigen, Switzerland	590 MeV	1.64 mA§	0.97 MW	Lead	—	Heavy water; cold source: liquid deuterium at 20 K
SNS	Short pulse	Oak Ridge National Laboratory, Oak Ridge, USA	1 GeV	1.4 mA	1.4 MW	Liquid mercury	60	2 × Water, 2 × liquid hydrogen

† Under construction. ‡ Currently operating at <0.5 MW. § Current reaching spallation target after attenuation in muon source.

Figure 2.3.12
Schematic diagram of the ESS facility. The proton beam enters at the right, strikes the target and liberates neutrons for instruments in the three neutron experiment halls. (Image courtesy of the ESS.)

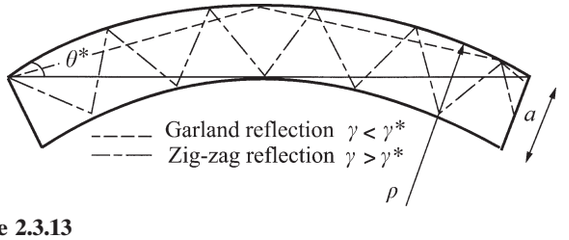

Figure 2.3.13
Plan of a curved neutron guide, indicating different possible neutron paths, labelled 'garland' and 'zig-zag'. Only the longer-wavelength neutrons can travel the zig-zag path because the glancing angles on this path (which must be less than the critical angle) are greater. In this schematic, the glancing angles, the width and the curvature have all been exaggerated. [From Section 4.4.2 of Volume C (Anderson & Schärpf, 2006).]

$$\lambda^* = \theta^* \left(\frac{\pi}{N b_{\rm coh}} \right)^{1/2}. \qquad (2.3.12)$$

This is known as the 'characteristic' wavelength of the guide [see Section 4.4.2 of Volume C by Anderson & Schärpf (2006)]; the majority of transmitted neutrons will have longer wavelengths than this.

The desire to use guides for shorter (*e.g.* thermal-neutron) wavelengths, and for retaining more neutrons at a given wavelength, has motivated the development of mirrors capable of reflecting neutrons incident at greater glancing angle. The earliest such mirrors were in fact monochromating mirrors obtained by laying down alternate layers of metals with contrasting coherent-scattering-length densities (Fig. 2.3.14). For a bilayer thickness d and angle of incidence θ these would select wavelengths according to Bragg's law [equation (1.1.3)],

$$\lambda = 2d \sin(\theta).$$

In an early implementation (Schoenborn *et al.*, 1974), the metals were Ge and Mn (which have coherent scattering lengths opposite in sign) and the bilayer thickness was of the order of 100 Å; this is a larger d-spacing giving access to longer wave-

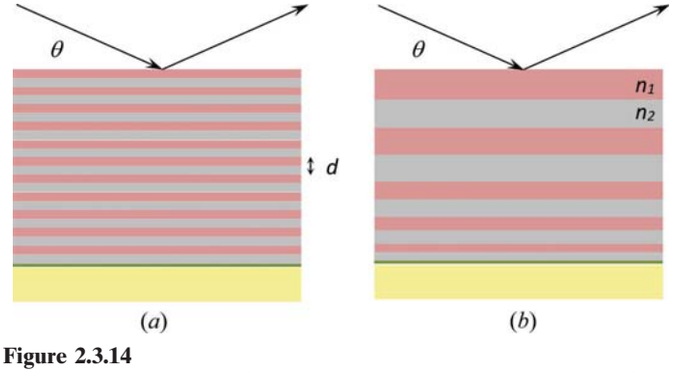

Figure 2.3.14
Schematic diagrams of (*a*) a multilayer monochromator and (*b*) a neutron supermirror.